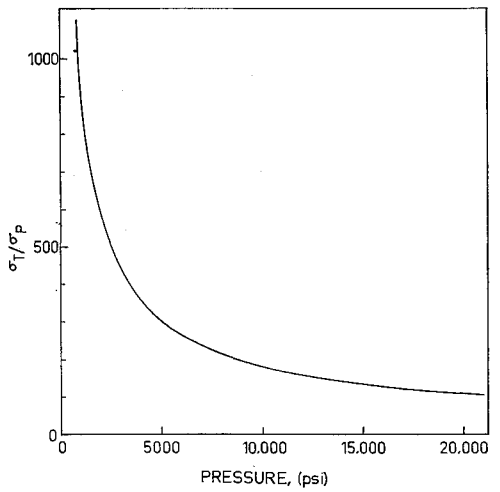

Fig. 3 Ratio of thermal stress to pressure stress at the surface of burning ammonium perchlorate as a function of pressure

σ_T/σ_P could be lowered sufficiently to make the effect of σ_P on cracking predominant.

It should be noted that in the previously proposed model[1] the expression for cracking velocity was

$$v = 2\alpha \sinh\beta P \tag{8}$$

where the constant β contains the arbitrary conversion constant n relating chamber pressure to the shear stress [Eq. (6)], which is responsible for cracking. The present analysis indicates that this stress arises from the pressure-dependent thermal gradient rather than from the pressure itself. Since the thermal stress is nearly linear in pressure for $P > 5000$ psi (Fig. 2), the model essentially is unaffected.

Certain factors not considered in the present treatment also may affect the cracking process. Crystal phase changes, with associated possible changes in crystal density (e.g., the change of orthorhombic to cubic AP at 240°C), may be involved in the cracking. This effect has been observed experimentally by Bowden and McAuslan in the thermal decomposition of silver azide.[3] Also, if the deflagrating material melts during decomposition, cracking may be *prevented*, either by relieving thermal stresses at the burning surface or by preventing penetration of hot gases into existing pores. The latter mechanism has been postulated by Taylor[8] to explain the absence of accelerated burning at low pressures in the burning of porous HMX charges.

References

[1] Irwin, O. R., Salzman, P. K., and Andersen, W. H., "Deflagration characteristics of ammonium perchlorate at high pressures," *Ninth Symposium (International) on Combustion* (Academic Press, New York, 1963).

[2] Friedman, R., private communication, Atlantic Research Corporation (August 1962).

[3] Bowden, F. P. and Yoffe, A. D., *Fast Reactions in Solids* (Academic Press Inc., New York, 1958); and Bowden, F. P. and McAuslan, F., "Slow decomposition of explosive crystals," Nature **178**, 408 (1956); also Evans, B. L. and Yoffe, A. D., "The burning and explosion of single crystals," Proc. Roy. Soc. (London) **238**, 325 (1957).

[4] Patry, M. and Lafitte, P., "Transition from burning to detonation in thin films," Compt. Rend. **193**, 171, 1339 (1931).

[5] Miller, D. R., "Friction and abrasion of hard solids at high sliding speeds," Proc. Roy. Soc. (London) **A269**, 368–384 (1962).

[6] Andersen, W. H. and Chaiken, R. F., "Detonability of solid composite propellants," ARS J. **31**, 1379–1387 (1961).

[7] Rosenthal, D., "The theory of moving heat sources," Trans. Am. Soc. Mech. Engrs. **68**, 849–866 (1946).

[8] Taylor, J. W., "The burning of secondary explosive powders by a convective mechanism," Trans. Faraday Soc. **58**, 561–568 (1962).

Initial Behavior of a Gun-Tunnel Piston

TAKEO SAKURAI*
Kyoto University, Kyoto, Japan

RECENTLY, the gun-tunnel has been used widely for the investigation of hypersonic flow. As is well known, it produces hypersonic flow with very high stagnation temperature by means of a piston motivated by the pressure difference between the high- and the low-pressure chambers. The behavior of the piston is essential to the performance of the apparatus, so that many studies of it have been made. Because of the mathematical difficulties, however, there is no analytical expression for the initial behavior of the piston. Hence, it will be interesting to obtain such an expression even for a very extreme condition. In this note the initial behavior of the gun-tunnel piston with a very small pressure difference is investigated by the small-perturbation method.

An infinitely long straight channel is divided by a diaphragm into high- and low-pressure chambers, and a piston is placed close to the diaphragm in the low-pressure chamber. The problem here is to discuss the behavior of the piston after bursting of the diaphragm within the small-perturbation method and without considering friction between the piston and the channel walls.

The basic equations of the one-dimensional unsteady motion of a compressible perfect fluid within the small-perturbation approximation are as follows:

$$P_i = P_{i0} + P_i' \qquad \rho_i = \rho_{i0} + \rho_i' \qquad U_i = u_i \tag{1}$$

$$P_i' = -\rho_{i0}\frac{\partial \varphi_i}{\partial t} \qquad \rho_i' = \frac{P_i'}{C_{i0}^2} \qquad u_i = \frac{\partial \varphi_i}{\partial x} \tag{2}$$

$$0 = [(\partial^2/\partial t^2) - C_{i0}^2(\partial^2/\partial x^2)]\varphi_i \tag{3}$$

where P, ρ, U, t, x, and C indicate the pressure, density, velocity, time, position, and sound speed, respectively. The subscripts 1, 2, and 0 indicate quantities in the high-pressure chamber, the low-pressure chamber, and the undisturbed state, respectively.

The initial conditions at the instant the diaphragm bursts are

$$P_1' = P_2' = 0 \qquad U_1 = U_2 = 0 \tag{4}$$

The boundary conditions on the piston are

$$u_1|_{x = f(t) - 0} = u_2|_{x = f(t) + 0} = f'(t) \tag{5}$$

$$mf'' = P_1 - P_2 \tag{6}$$

where m is the mass of the piston and $x = f(t)$ describes the locus of the piston in the (x, t) plane. The last equation is simply the equation of motion for the piston.

The general solution of the wave equation (3) can be obtained as follows:

$$\varphi_i = F_i(x + C_{i0}t) + G_i(x - C_{i0}t) \tag{7}$$

Substituting (7) into the initial conditions (4), it can be shown that φ_1 and φ_2 are both zero below the wave front in Fig. 1, i.e., the fluid in both the high- and the low-pressure chambers is not disturbed until the wave front reaches it. Then, by the continuity of the potential on the wave front, the solution in the region between the wave front and the piston can be obtained as follows:

$$\varphi_1 = F_1(x + C_{10}t) \tag{8}$$

Received by IAS July 2, 1962. The author wishes to express his cordial thanks to J. B. Tiedemann for his kind inspection of the manuscript of this note.

* Assistant Professor, Department of Aeronautical Engineering, Faculty of Engineering.

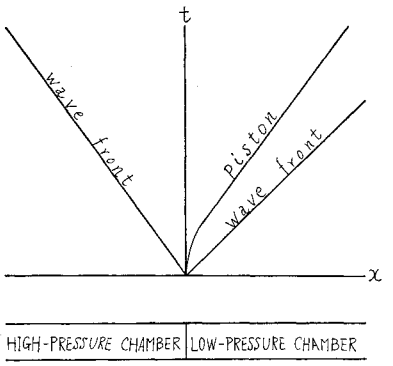

Fig. 1 x, t plane of the motion

$$\varphi_2 = G_2(x - C_{20}t) \tag{9}$$

Substituting the foregoing into the boundary conditions (5) and (6) and using the basic relations (1) and (2), the following equations are obtained:

$$F_1'[f(t) + C_{10}t] = f'(t) \tag{10}$$

$$G_2'[f(t) - C_{20}t] = f'(t) \tag{11}$$

$$mf''(t) = P_{10} - P_{20} - \rho_{10}C_{10}F_1'[f(t) + C_{10}t] - \rho_{20}C_{20}G_2'[f(t) - C_{20}t] \tag{12}$$

Eliminating F_1 and G_2 from the preceding equations, one obtains an ordinary differential equation of the first order for $f'(t)$:

$$mf'' + (\rho_{10}C_{10} + \rho_{20}C_{20})f' = P_{10} - P_{20} \tag{13}$$

The initial condition for $f'(t)$ is obtained from conditions (4) and (5) as follows:

$$f'(0) = 0 \tag{14}$$

The solution of differential equation (13) satisfying the initial condition of Eq. (14) can be obtained easily to give

$$f' = \frac{P_{10} - P_{20}}{\rho_{10}C_{10} + \rho_{20}C_{20}}\left[1 - \exp\left(-\frac{\rho_{10}C_{10} + \rho_{20}C_{20}}{m}t\right)\right] \tag{15}$$

If a light piston is used, the piston speed approaches the final speed very rapidly, as is expected intuitively. On the other hand, the final speed is independent of the piston mass and depends only on the pressure difference between the high- and low-pressure chambers and state of the gas in both chambers. The pressures on the front and rear surfaces of the piston are, of course, equal in the final state to the average of P_{10} and P_{20}.

Effective Displacement Thickness for Boundary Layers with Surface Mass Transfer

WESLEY M. MANN JR.*
Aerospace Corporation, El Segundo, Calif.

Nomenclature

u = velocity component parallel to surface in stream direction
v = velocity component normal to surface
x = coordinate parallel to surface in stream direction
y = coordinate normal to surface
y_c = height of control surface, const
δ = total boundary layer thickness

Received December 20, 1962.

* Member of the Technical Staff, Engineering Division. Member AIAA.

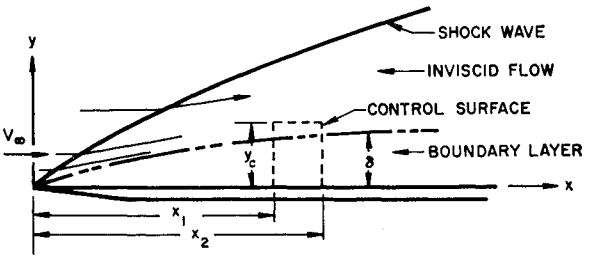

Fig. 1 Flow model

δ^* = boundary layer displacement thickness [defined by Eq. (2)]
Δ^* = effective displacement thickness [defined by Eq. (8)]
θ = flow angle, $\tan^{-1}(v/u)$
ρ = mass density

Subscripts

e = flow conditions external to the boundary layer
w = wall conditions

THE foundation of the well-known strong and weak viscid-inviscid interaction theories due to Lees and Probstein[1, 2] rests on the assumptions that 1) the boundary layer is separated from the shock wave by an inviscid shock layer; 2) classical boundary layer theory can be applied; and 3) the local steamwise variation in pressure and other flow properties can be calculated if the deflection or displacement of the inviscid flow due to the presence of the boundary layer is known.

The flow external to the boundary layer is calculated by an appropriate inviscid-flow theory for a fictitious body that has a thickness equal to that of the original body plus an additional thickness to account for the displacement effect of the boundary layer. When the tangent-wedge approximation is used for the inviscid solution, the original body slope is increased by the rate of change of the boundary layer displacement effect.

This note employs a continuity argument to derive this displacement effect for a boundary layer with surface mass transfer for application to the calculation of viscid-inviscid interaction on ablating or transpiration-cooled surfaces. The flow model used is given in Fig. 1. In order to avoid direct involvement with the rather nebulous concept of total boundary layer thickness δ, the control surface, detailed in Fig. 2, was chosen with a constant height $y_c > \delta$, such that,

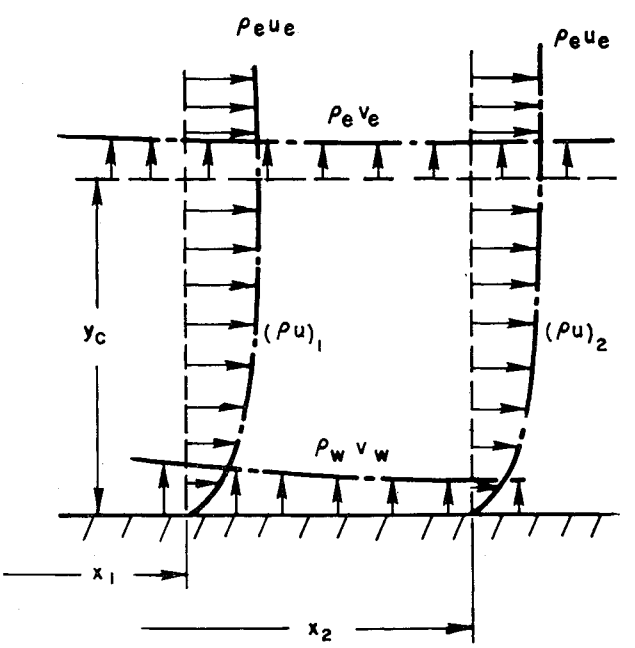

Fig. 2 Mass flow through the control surface